Universidad de los Llanos

ORINOQUIA REVISTA
Suplemento Volumen 25 - Número 1, Enero-Junio 2021

Artículo original/Original Article

Photon Harvesting Molecules: Ionization Potential from Quantum Chemical Calculations of Phytoplanktonic Pigments for MALDI-MS Analysis

Moléculas captadoras de fotones: potencial de ionización de pigmentos fitoplanctónicos a partir de cálculos de química cuántica para análisis MALDI-MS

Moléculas de coleta de fótons: potencial de ionização a partir de cálculos químicos quânticos de pigmentos fitoplanctônicos para análise de MALDI-MS

Recibido: 24 de noviembre de 2020. **Aceptado**: 13 de mayo de 2021.

***Carlos A. Padilla-Jaramillo*[1],**
Biol.; https://orcid.org/0000-0003-3577-3460

***Luis M. Díaz-Sánchez*[2],**
Quim, MSc; https://orcid.org/0000-0002-2748-9374

***Marianny Y. Combariza-Montañez*[2**],**
B.S, MSc, PhD; https://orcid.org/0000-0002-6907-4759

Cristian Blanco-Tirado*[2],**
B.S, MSc, PhD; https://orcid.org/0000-0002-3650-5487

***Aldo F. Combariza-Montañez*[1*],**
Ing. Quim, MSc, PhD;
https://orcid.org/0000-0003-4837-7723

[1] Molecular Modeling and Computational Simulation - in silico Research Group, Departamento de Biología y Química, Universidad de Sucre, Sincelejo, Sucre, Colombia. (700001-Urb.)
Email: carlos.padilla@unisucrevirtual.edu.co
[*] Email: aldo.combariza@unisucre.edu.co
[2] Escuela de Química, Universidad Industrial de Santander (UIS), Bucaramanga, Santander, Colombia. 680003.
Email: luismiguellmds@gmail.com
[**] Email: marianny@uis.edu.co
[***] Email: cblancot@uis.edu.co

Suplemento Orinoquia, Enero-Junio 2021; 25(1): 13-23
ISSN electrónico: 2011-2629
ISSN impreso: 0121-3709
https://doi.org/10.22579/20112629.676

Abstract

The Ionization Potential (IP) of chemical species is of paramount importance for the Matrix Assisted Laser Desorption/Ionization (MALDI) analytical technique. Specifically, IPs are used in MALDI MS Electron Transfer (ET) as a parameter to select the matrix for a given family of chemical species. We used a quantum chemical methodology to computationally determine IPs for a set of photosensible phytoplanktonic pigments. These calculations could be used as a guide for MALDI matrix selection. IPs were determined using Koopman's Theorem, via Geometry Optimization and Single Point Energy within the Restricted Closed-Shell Hartree-Fock (RHF) technique. Structures of a twenty-four set of pigments were geometrically optimized, and their IPs determined. Calculated IP's are in close agreement to reported experimental IPs within an average 3.7% absolute error. Structural features of the chemical species studied have a closed relationship with their chemical properties and IP's. Our results suggest that ET-MALDI matrices such as DCTB (IP = 8.5 eV) and CNPV-OCH_3 (IP = 8.3 eV) could be more suitable to analyze these types of chemical species.

Keywords: *Koopsman, Hartree-Fock, HOMO-energy, Pigments, MALDI-MS, Electron-Transfer.*

Resumen

El Potencial de Ionización (PI) de especies químicas es de vital importancia en técnicas de química analítica como Matrix-Assisted Laser Desorption/Ionization (MALDI). Específicamente, el cálculo de PI es usado rutinariamente en MALDI con matrices de Transferencia Electrónica (TE) para la selección de la matriz adecuada para una familia de especies químicas. En este estudio se usaron metodologías computacionales basadas en la mecánica cuántica para determinar teóricamente los PIs de un grupo de pigmentos fotosensibles provenientes del fitoplancton y así poder realizar de forma más acertada el proceso de selección de matrices MALDI. Los PIs fueron determinados usando el teorema de Koopmans a través de Optimizaciones Geométricas y cálculos de Single Point Energy (SPE) con nivel de teoría Hartree-Fock de capa cerrada (RHF). Las estructuras de 24 pigmentos fueron optimizadas y sus PIs fueron determinados. Los valores de PIs calculados están muy cercanos a los reportes experimentales de la literatura, con un porcentaje de error absoluto aproximado de 3,7% y con cambios estructurales relacionados con las propiedades químicas de los pigmentos y IPs. A partir de nuestros resultados,

Como Citar (Norma Vancouver):
Padilla-Jaramillo CA, Combariza-Montañez MY, Blanco-Tirado C, Combariza-Montañez AF. Photon Harvesting Molecules: Ionization Potential from Quantum Chemical Calculations of Phytoplanktonic Pigments for MALDI-MS Analysis. Orinoquia,2021;25(Suplemento 1):13-23. https://doi.org/ 10.22579/20112629.676

se sugiere que algunas matrices MALDI ET tales como la DCTB (PI = 8,5 eV) y CNPV-OCH3 (PI = 8,3 eV), podrían ser las más adecuadas para ser usadas con esta familia de compuestos.

Palabras clave: *Koopsman, Hartree-Fock, Energía-HOMO, Pigmentos, MALDI-MS, Transferencia-Electrónica.*

Resumo

O potencial de ionização (PI) de espécies químicas é de suma importância nas técnicas de química analítica como o Matrix-Assisted Laser Desorption/Ionization (MALDI). Especificamente, o cálculo de PI é usado em ensaios MALDI com matrizes de transferência eletrônica (TE) para conseguir selecionar uma matriz adequada para analisar uma família de espécies químicas em particular. Neste estudo foram usadas metodologías computacionais baseadas na mecânica cuántica para determinar teóricamente os PI de um grupo de pigmentos fotossensíveis do fitoplâncton, e assim realizar de forma mais acurada o processo de seleção de matrizes MALDI. Os PI foram determinados usando o teorema de Koopmans através de otimizações geométricas e cálculos de Single Point Energy (SPE) com nível de teoria de Hartree-Fock de casca fechada (RHF). As estruturas dos 24 pigmentos foram otimizados e seus PI foram determinados. Os valores de PI calculados estão muito próximos aos informes experimentais na literatura, com uma porcentagem de erro absoluto aproximado de 3,7% e as mudanças estruturais têm uma relação próxima com as propriedades químicas dos pigmentos, especialmente seus PI. Algumas matrizes MALDI-ET tais como DCTB (PI = 8,5 eV) e CNPV-OCH3 (PI = 8,3 eV) podem ser usadas para analisar estes pigmentos.

Palavras-chave: *Teorema de Koopmans, Hartree-Fock, Energia-HOMO, Pigmentos, MALDI-MS, transferência eletrônica.*

Introduction

Phytoplankton constitute an essential component in aquatic ecosystems, shaping the base of the food chain pyramid and building up for at least a quarter of the world biomass (Olenina *et al.*, 2006; Roy *et al.*, 2012). Phytoplanktonic species are the pioneer photosynthetic organisms/producers in all ecosystems, generating complex carbon compounds from carbon dioxide (CO_2) and using sunlight as energy source for the metabolic processes (Bellinger and Sigee, 2015; Burneo and Romero, 2016). Specifically, photosynthetic residues coming from their metabolism generates about 50% of primary mass (organic matter) on the planet, keeping the ecological balance of dissolved nutrients in water sources (Descy and Gosselain, 1994; Field, 1998).

Photosynthetic processes are carried out by complex biochemical photosystems (PS), specifically the PSI and PSII, which harvest sunlight energy in a highly efficient way in order to keep the homeostasis. These PS's are located inside chloroplast thylakoid membranes (Burneo and Romero, 2016; Beardall, 1989). PSI and PSII complexes are of three types: chlorophylls, carotenoids and phycobilins, present in different combinations and proportions (Bellinger and Sigee, 2015; Golbeck and van der Est, 2014). Some particular pigments such as **α**-carotene, λ-carotene and ε-carotene are present only in particular phytoplanktonic species, which gives them the potential to be used as chemotaxonomic markers (Roy *et al.*, 2012; Takaichi, 2011). Mass Spectrometry (MS) has been reported as a technique useful to study these pigments, and, specifically Electron Transfer (ET) coupled to Matrix Assisted Laser Desorption/Ionization (MALDI) source, has been recognized as an excellent option for analyzing these compounds (Sánchez, 2019). In this regard, ET MALDI has proven more accurate and straightforward, compared to other techniques, such as High Performance Liquid Chromatography (HPLC) (Sánchez, 2019; Siuzdak, 2004).

In ET MALDI MS, the Ionization Potential (IP) is one of the most sensitive physical chemistry parameters to calculate, which allows to explain the ET process between analyte and matrix (Castellanos-García *et al.*, 2015; Castellanos-García *et al.*, 2017; Ramírez-Pradilla *et al.*, 2019.a; Ramírez *et al.*, 2019). Also, it is of paramount importance to guarantee a larger value for the matrix IP, compared to the analyte, in order to achieve charge migration (see Eq. 3) (Vasil'ev *et al.*, 2006; Persico and Granucci, 2018; Robb, 2018).

$$Matrix + h\upsilon \rightarrow Matrix^{*}(E = h\upsilon) \tag{1}$$

$$Matrix^{*} \rightarrow Matrix^{+\cdot} + e^{-}(E > IP_{Matrix}) \tag{2}$$

$$Matrix^{+\cdot} + Analyte \rightarrow Matrix + Analyte^{+\cdot}(IP_{Matrix} > IP_{Analyte}) \tag{3}$$

The number of experimental IPs reported in the scientific literature for phytoplanktonic pigments is very limited and quite outdated (Nakato *et al.*, 1974; Goupy *et al.*, 2018). On the other hand, IPs reported from theoretical studies are more recent but also reduced in quantity (Jaramillo *et al.*, 2012; Hasegawa and Noguchi, 2005). Therefore, we point our efforts to develop a computational protocol to predict IPs of photosensible phytoplanktonic pigments by applying the Koopmans theorem *via* quantum chemical calculations (Koopmans, 1934; Ramachandran *et al.*, 2008; Jensen, 2017). In order to evaluate the quality of our results, we will use a set of experimentally measured IPs and also data coming from ET MALDI performed at our laboratory (Giraldo-Dávila *et al.*, 2018; Castellanos-García *et al.*, 2017; Ramírez-Pradilla *et al.*, 2019.a; Ramírez-Pradilla *et al.*, 2019.b). Our results will allow us to make a more reliable MALDI matrix selection suitable for a specific family of chemical species, such as those coming from phytoplanktonic species.

Methods and Materials

Computational Resources and Software

Quantum chemical calculations were executed using the *ab initio* quantum chemistry program ORCA (Neese, 2018-2020), using the facilities of the High Performance Computing Cluster INKARI, located in the “Instituto Astronómico y Aeroespacial Pedro Paulet”, Universidad Nacional de San Agustín, Arequipa, Perú (http://inkari.iaapp.edu.pe/).

Geometry optimizations were carried out within the Restricted Closed-Shell Hartree-Fock (RHF) method, increasing the size of the basis set from STO-3G, def2-SVP and def2-TZVP (Hartree, 1928; Fock, 1930; Gomez *et al.*, 2009). A total of 24 photosensible phytoplanktonic pigments taken from PubChem (https://pubchem.ncbi.nlm.nih.gov/) and ChemSpider (http://www.chemspider.com/) databases were analyzed: 7 chlorophylls and 17 carotenoids and xanthophylls (See Table 1).

The RHF method uses the both, Born-Oppenheimer and the independent-particle approximations to build the Hamiltonian operator and the wave function of any molecular system (Ramachandran *et al.*, 2008; Lewars, 2011). This wavefunction is based on the Linear Combination of Atomic Orbitals (LCAO) method, which represents a molecular orbital (Lewars, 2011). The HF equation is described as:

$$\hat{F}_i \phi_i' = \hat{\epsilon}_i \phi_i' \qquad (4)$$

where the $\hat{F}_i$ is the Fock operator, ϕ_i' is the wavefunction and $\hat{\epsilon}_i$ is the energy. On the other hand, the basis set STO-3G is a minimum basis set and the def2-SVP and def2-TZVP are extended.

Koopmans theorem

IPs were determined by applying the Koopmans theorem for closed-shell molecular systems. This theorem states that the first ionization energy equals the negative value of the HOMO frontier orbital energy, within the RHF method (Ramachandran *et al.*, 2008). Mathe-

Table 1. Molecular species analyzed. **Source:** Authors.

Pigment name	Molecular Weight (u)	Chemical formula	Pigment name	Molecular Weight (u)	Chemical formula
4,4′-Diapolycopenedial	428.6056	$C_{30}H_{36}O_2$	**Diadinoxanthin**	582.855	$C_{40}H_{54}O_3$
Alloxanthin	564.8397	$C_{40}H_{52}O_2$	**Neoxanthin**	600.8702	$C_{40}H_{56}O_4$
Astaxanthin	596.8385	$C_{40}H_{52}O_4$	**Peridinin**	630.8101	$C_{39}H_{50}O_7$
Antheraxanthin	596.8385	$C_{40}H_{56}O_3$	**Zeaxanthin**	568.8714	$C_{40}H_{56}O_2$
Astacene	592.8067	$C_{40}H_{48}O_4$	**Diatoxanthin**	566.8556	$C_{40}H_{54}O_2$
α-Carotene	536.8726	$C_{40}H_{56}$	**Chlorophyll a**	893.489	$C_{55}H_{72}MgN_4O_5$
β-Carotene	536.8726	$C_{40}H_{56}$	**Chlorophyll b**	907.4725	$C_{55}H_{70}MgN_4O_6$
β-Cryptoxanthin	552.872	$C_{40}H_{56}O$	**Chlorophyllide a**	614.9733	$C_{35}H_{34}MgN_4O_5$
Crocoxanthin	550.8562	$C_{40}H_{54}O$	**Chlorophyll c1**	610.9415	$C_{35}H_{30}MgN_4O_5$
Canthaxanthin	564.8397	$C_{40}H_{52}O_2$	**Chlorophyll c2**	608.9256	$C_{35}H_{28}MgN_4O_5$
Lutein	568.8714	$C_{40}H_{56}O_2$	**Pheophorbide a**	592.6841	$C_{35}H_{36}N_4O_5$
Fucoxanthin	658.9063	$C_{42}H_{58}O_6$	**Pheophorbide b**	606.6677	$C_{35}H_{34}N_4O_6$

matically, the koopmans theorem is represented by the equations 5 and 6.

$$E_N - E_{N-1} = h_k + \frac{1}{2}\sum_{i=1}^{N_{elec}}(J_{ik}) - K_{ik} + \sum_{j=1}^{N_{elec}}(j_{ij} - K_{ij}) \qquad (5)$$

$$E_N - E_{N-1} = h_k + \sum_{i=1}^{N_{elec}}(J_{ik}) - K_{ik}) = \epsilon_k \qquad (6)$$

where, equation 6 shows that EN – EN – 1 is equal to the $\in_k$ energy in Eq. 4.

Results

The geometry optimization of the selected set of chemical species was carried out within the RHF level of theory using the def2-TZVP basis set and the optimized configurations are shown in figure 1. The highlighted regions of the optimized configurations show the largest structural deviations compared to the initial structures.

Figure 2 clearly shows stabilization in molecular energy as early as the second optimization step. For all structures, the minimization curve flattens rapidly, *i.e.*, the molecular energy stabilizes. Only some particular pigments such as Chlorophyll c2 (Chl_c2), Chlorophyllide a, Diatoxanthin, Piridinin, Fucoxanthin and 4,4'-Diapolycopenedial are exceptions. The associated Single Point Energy (SPE) calculation for each pigment

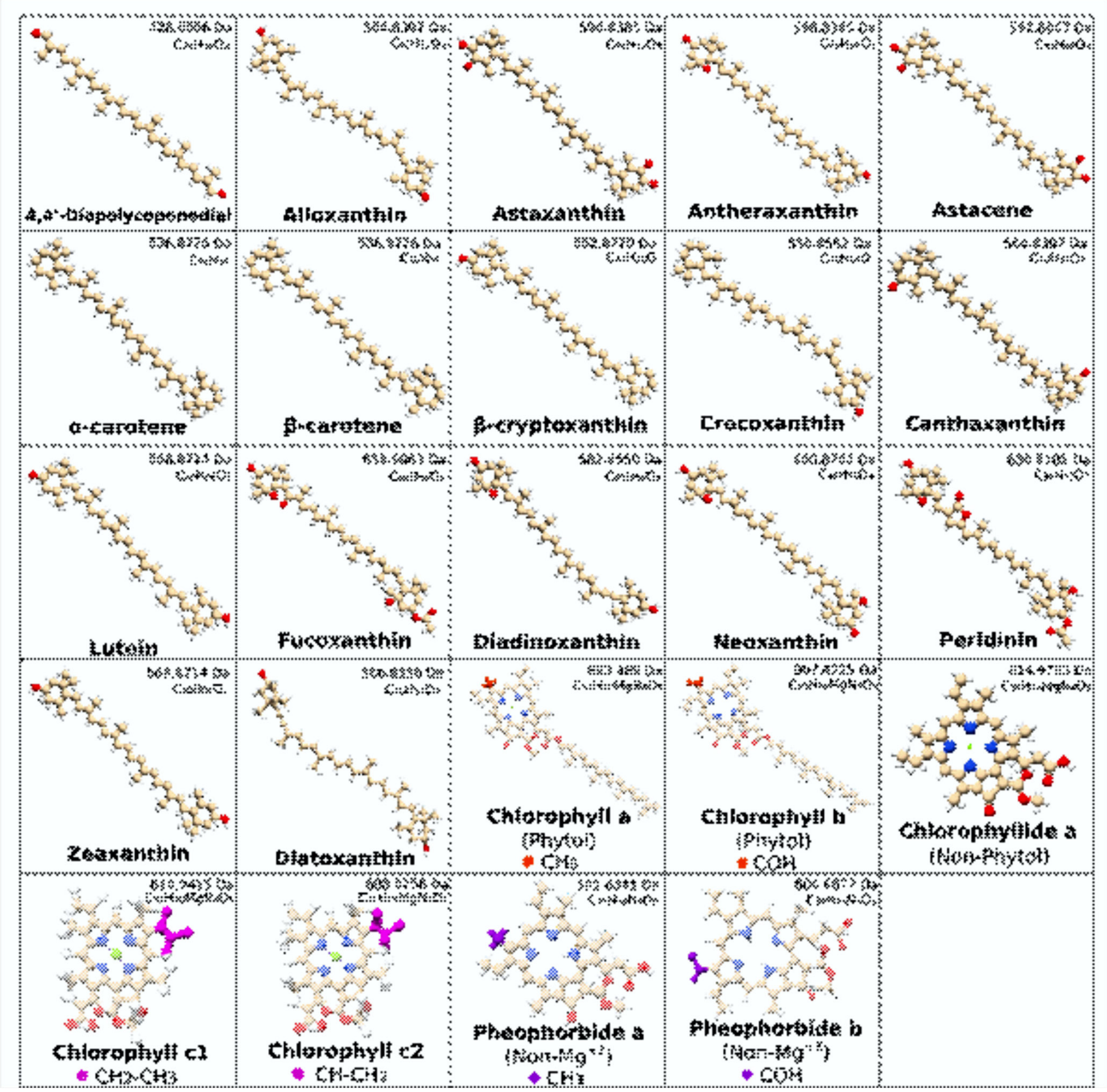

Figure 1. Chlorophyll, carotenoid and xanthophyll molecular structures (ball and stick model): minimized geometries. **Source:** Authors.

final configuration is shown in figure 2. From these molecular conformations we extracted the ionization energies by applying the Koopman's theorem, that is, by taking the negative value of the HOMO energy for each molecule.

HOMO frontier orbitals were drawn for each molecule. The HOMO shows the probability regions for the external shell electrons in the molecules, which are responsible for the chemical interactions with the matrix along the ET process. For the chlorophyll family, HOMO orbitals are located on the porphyrin rings; while, for the carotenoids (xanthophylls and carotenes) HOMO orbitals are located inside the molecule core (See Figure 3).

Calculated IPs were compared to experimental IPs reported in the literature, when existing data is available, as reported in Table 2. Comparison of IP's show that calculated energies overestimate experimental values, with a relatively small deviation of ~3.7% (see Figure 4). Lutein and Canthaxanthin IPs show the lowest error compared to experimental reports, with 1.5% and 2.0% for Lutein and Canthaxanthin respectively. Chl_c2 and α-carotene show the largest deviation from experiments, with 7.52 and 6.20% respectively (See Table 2).

An interesting behavior is observed for the calculated IPs of similar structures. A particular substitution of the -CH_3 (methyl) in Chl_a for -COH (aldehyde) in Chl_b, causes an IP difference of 0.42 eV, whereas a more sizable structural change between Chl_a and Chlorophyllide_a, where the phytol tail is removed, shows a small variation in IP of 0.08 eV. Between Chlorophyllide_a and Chlorophyll c1 (Chl_c1) structures does not occur atom substitution, but Chl_c1 has an additional double-bound compared to the Chlorophyllide_a, which produces a ΔIP = 0.2 eV (see Figure 1). The difference could be ascribed to the presence of the double-bond.

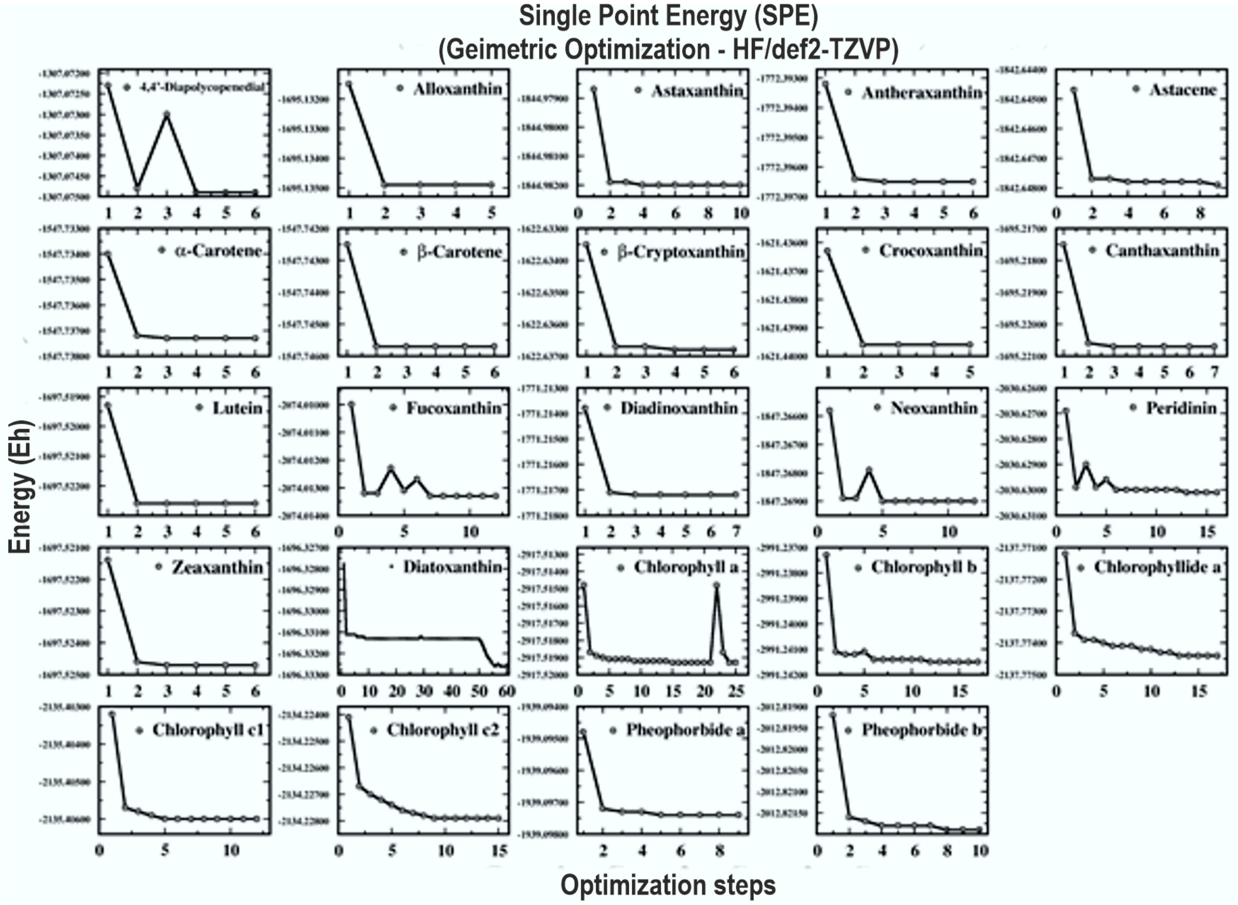

Figure 2. Single point energy of Photosensible pigments from structural optimization with HF/def2-TZVP. **Source:** Authors

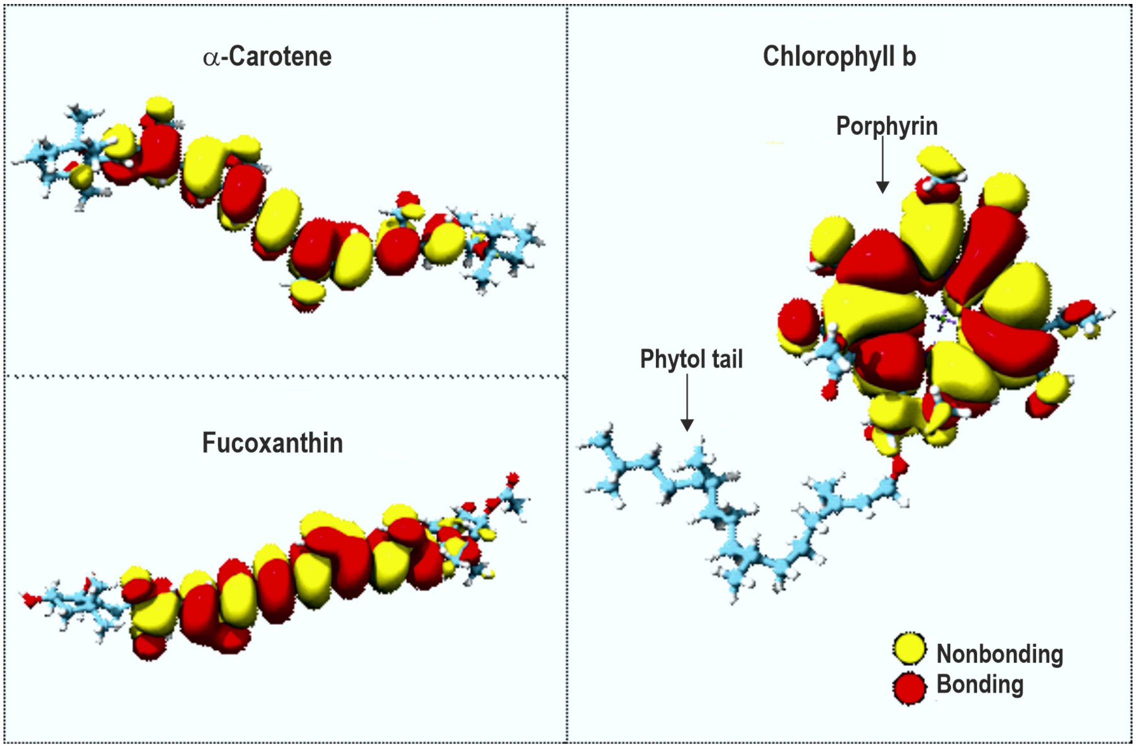

Figure 3. HOMO orbitals of chlorophyll and carotenoids. **Source**: Authors.

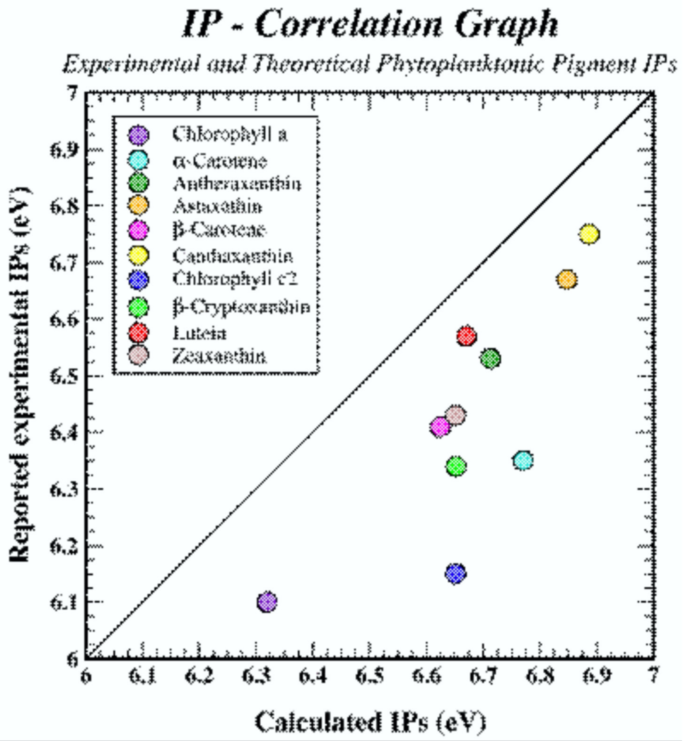

Figure 4. Correlation between reported experimental IPs and calculated IPs. **Source:** Authors.

The $-CH_2-CH_3$ functional group in the Chl_c1 molecule is substituted to $-CH=CH_2$ in the Chl_c2 molecule (see Figure 1). The Chl_c2 presents a double bond and the loss of two hydrogen atoms with respect to the Chl_c1 molecule, which generates an IP difference of 0.05 eV. This Chl_c1-Chl_c2 case is similar to Chl_c1-Chlorophyllide_a structural change. However, the Chl_c1-Chl_c2 case has a loss of one hydrogen atom more than the Chl_c1-Chlorophyllide_a case. Additionally, the chemical environment in the site of substitutions is different. Between Pheo_a and Chlorophyllide_a, the only structural difference is the presence of an Mg^{+2} central atom forming four coordinated bonds with Nitrogen (N), which makes an IP difference of 0.4 eV. Thus, the Mg^{+2} atom absence increases the IP value. Finally, in the group of chlorophyll pigments, the substitution of $-CH_3$ group to $-HC=O$ group in the Pheophorbide_b (Pheo_b) from Pheo_a structure, causes a **Δ**IP of 0.27 eV. The carotene and xanthophyll molecules present a similar behavior of structure-IP relationship compared with the chlorophyll mentioned above, i.e., the presence of double bonds or functional groups with oxygen atoms in a determined position increases or decreases the IP value in the molecules.

All carotene and xanthophyll molecules exhibit similar structures and these compounds contain only Carbon (C), Oxygen (O) and Hydrogen (H) atoms (Roy

Table 2. Calculated and reported experimental IPs **Source:** Authors.

Pigment name	Calculated IP (eV)	Reported experimental IP (eV)	ΔIP (eV)	Error (%)
4,4′-Diapolycopenedial	6.70			
Alloxanthin	6.72			
Astaxanthin	6.85	6.67 ± 0.1 (Goupy *et al.*, 2018)	0.18	2.63
Antheraxanthin	6.71	6.53 ± 0.1 (Goupy *et al.*, 2018)	0.18	2.68
Astacene	7.07			
α-Carotene	6.77	6.35 ± 0.1 (Goupy *et al.*, 2018)	0.42	6.20
β-Carotene	6.62	6.41 ± 0.1 (Goupy *et al.*, 2018)	0.21	3.17
β-Cryptoxanthin	6.65	6.34 ± 0.1 (Goupy *et al.*, 2018)	0.31	4.66
Crocoxanthin	6.66			
Canthaxanthin	6.89	6.75 ± 0.1 (Goupy *et al.*, 2018)	0.14	2.03
Lutein	6.67	6.57 ± 0.1 (Goupy *et al.*, 2018)	0.10	1.50
Fucoxanthin	7.03			
Diadinoxanthin	6.80			
Neoxanthin	6.78			
Peridinin	6.87			
Zeaxanthin	6.65	6.43 ± 0.1 (Goupy *et al.*, 2018)	0.22	3.31
Diatoxanthin	6.72			
Chlorophyll a	6.32	6.1 ± 0.2 (Nakato *et al.*, 1974)	0.22	3.48
Chlorophyll b	6.74			
Chlorophyllide a	6.40			
Chlorophyll c1	6.60			
Chlorophyll c2	6.65	6.15 ± 0.2 (Jaramillo *et al.*, 2012)	0.45	7.52
Pheophorbide a	6.80			
Pheophorbide b	7.07			

et al., 2012). Specifically, the main difference between carotenoid and xanthophyll molecules is the presence of oxygen atoms in the xanthophyll structures. The two carotenes studied here were the *α*-carotene and *β*-carotene, which have an IP difference of 0.15 eV between them. To evaluate the presence of Oxygen atoms in the hydrocarbon structures, the comparison of structures and IP values between the Alloxanthin and *α*-carotene or *β*-carotene molecules is ideal, because the only structural change is the presence of an -OH group in the Alloxanthin molecule (see Figure 1). The *α*-carotene IP value is 6.77 eV and the IP value of Alloxanthin pigment is 6.72 eV. Another good example of IP-structure relation is the comparison between Lutein and Canthaxanthin, where Lutein has an alcohol group, while the Canthaxanthin molecule has the carbonyl group, causing significant IP changes. Our preliminary results show that the presence of double or triple bonds causes a small increase of IP energies, such as in Crocoxanthin and *β*-Cryptoxanthin molecules (See Figure 1 and Table 2).

Discussion

The overestimation of IPs with respect to experimental data can be explained by the mathematical approximations made in the RHF level of theory used to solve the Time-Independent Schrödinger equation (Jensen, 2017). The main approximation is the Born-Oppenheimer (BO), which says that the electron and nuclear motions can be considered separately, because the nuclear motion is rather small, compared to that of the electrons. Therefore, the nuclei are statics (Born and Oppenheimer, 1927). And the second approximation made in the HF method is the Independent-Particle approximation, which says that the electronic correlation is not considered as a particular mathematical term in the solution, it is taken as an average value (Jensen, 2017). These two approximations cause systematic errors and the underestimation of the calculated energies.

On the other hand, in the Koopmans theorem, the frozen orbital approximation assumes that the N±1-electron state (positive or negative ion) is equal to the N-electron state, neglecting the spin-orbital relaxation and producing overestimations in the IP values (Müller, 1980; Szabo and Ostluand, 1996; Plakhutin, 2018). The systematic errors mentioned above, Independent-Particle and frozen orbital approximations, cancel each other and generate good IP results. Therefore, the obtained IP errors are considered as a typical and expected result.

The IP variations due to structural changes can be explained by several chemical factors such as the mesomeric effect caused for the functional groups and the electronegative and electropositive tendencies in the molecules (Lazzari-Dean, 2015). The increase of IP value in the Pheo_b molecule to Pheo_a and in the Chl_a to Chl_b molecule, due to the substitution of $-CH_3$ to -HC=O functional group can be explained by the presence of the carbonyl group (C=O). The C=O is an electron-withdrawing group; therefore, compounds with this functional group tend to attract electrons and their IP value increases (Lazzari-Dean, 2015; Szent-Györgyi, 1968; Tian *et al.*, 2010), the carbonyl group, C=O, being the main carbonyl group of ketones or aldehydes (Szent-Györgyi, 1968). Contrarily, the -OH functional group in the Alloxanthin causes an IP reduction with respect to *α*-carotene, as mentioned above. The -OH group is an electropositive compound, *i.e.*, an electron donor, therefore the energy to remove an electron is lower (the mesomeric effect is positive, +M) (Szent-Györgyi, 1968; Triggle and Taylor, 2006; Tian *et al.*, 2010). Indeed, the presence of a double or triple bond causes a **Δ**IP lower than that caused only for the presence of oxygen atoms or another substitute. These ϖ-bonds involve ϖ-electron delocalization which contributes to changes in the electron attraction or repulsion (Triggle and Taylor, 2006). An example of this behavior is of *β*-cryptoxanthin and Crocoxanthin, where the **Δ**IP between them is only 0.01 eV, showing Crocoxanthin a triple bond. For the carotenoid pigments, in the conjugated cycle systems, it is clear how the functional group position impacts the IP value. The -ortho, -para, or -meta positions change the chemical electron donor or attraction properties (Lazzari-Dean, 2015). Specifically, the -OH functional group in the meta position generates larger IP relative to the -ortho and -para positions.

Concerning the IP values only, some ET MALDI matrices such as the trans-2-[3-(4-tert-Butylphenyl)-2-methyl-2-propenylidene]malononitrile (DCTB) (IP = 8.54 eV) (Ulmer *et al.*, 2000) or ET matrices based on Phenylenevinylene (PV) and fluorenone cores such as $CNPV-OCH_3$ (IP = 8.3 eV) (Castellanos-García *et al.*, 2017; Ramírez-Pradilla *et al.*, 2019.a; Godoy *et al.*, 2019; Cristancho *et al.*, 2016) can efficiently be used to analyze phytoplanktonic pigments. A preponderant requirement for the suitable charge migration, is that the IP differences between Matrix and Analyte should be larger than 0.5 eV (McCarley *et al*,. 1998).

Conclusions

Computationally calculated IP's are of paramount importance for ET MALDI matrix selection. We have successfully calculated IP's for a set of phytoplanktonic compounds: chlorophylls (7), carotenoids (2) and xanthophylls (15); with very close agreement to experimental results at relatively low computational cost, on average 9.4 hours/system. For the purpose of this research IP errors obtained are in excellent agreement with experimental values. The computational approach described here allows to ascribe IPs differences to structural changes and to the presence of particular functional groups, showing the intimate relationship structure and physical plus chemical properties. From the calculated IP values, we can suggest advantages on some ET MALDI matrices reported in the literature for ET analysis, specifically for phytoplanktonic photosensible pigments. We are working on improving this methodology, using alternatives to the Koopman's theorem to overcome the approximations involved in the RHF method.

Acknowledgements

We acknowledge the National University of San Agustín (UNSA, Arequipa, Perú) for providing access to INKARI (High Performance Computer Facilities, located at the Astronomical Observatory of CHARACATO - UNSA, Arequipa, Perú). Also, AFC acknowledges Dr. Wilson M. Castro Silupu for building scientific cooperation bridges UNSA-UNISUCRE, to M.Sc. Wilder Nina C. for technological support, and Dr. Luz E. De La Ossa for gently lending a hand with the manuscript. AFC and CAP acknowledge research exchange program by Universidad Industrial de Santander (UIS) and Experimental and Theoretical Physical Chemistry Research Group (GIFTEX). Also, to all members of GIFTEX and IN SILICO research groups for their constant collaboration and advice. Thanks to Guatiguara Technology Park and the Central Research Laboratory Facility at Industrial University of Santander for infrastructural support. We also acknowledge a graduate fellowship and financial support from SGR- BPIN: 2019000100020.

References

Beardall J. Photosynthesis and photorespiration in marine phytoplankton. *Aquatic Botany*. 1989;34(1-3):105-130. https://doi.org/10.1016/0304-3770(89)90052-1

Bellinger EG, Sigee DC. (2015). Freshwater Algae: Identification, Enumeration and use as Bioindicators (2nd ed.). Wiley BlackWell.

Born M, Oppenheimer R. Zur Quantentheorie der Molekeln. *Annalen Der Physik*. 1927;389(20):457-484. https://doi.org/10.1002/andp.19273892002

Burneo MCG, Romero NPG. Catálogo de microalgas y cianobacterias de agua dulce del ecuador: Biodiversidad de los principales géneros de microalgas y cianobacterias encontradas en sistemas lacustres de áreas protegidas de los andes y amazonía del ecuador. *In Anales de Medicina Interna*. 2016;6(12).

Castellanos-García L, Combariza M, Blanco-Tirado C. (2015). Desarrollo de una matriz para espectrometría de masas MALDI basada en sistemas tipo fenilenvinileno y ácidos acrílicos. Universidad Industrial de Santander.

Castellanos-García LJ, Agudelo BC, Rosales HF, Cely M, Ochoa-Puentes C, Blanco-Tirado C, et al. (Oligo p-Phenylenevinylene Derivatives as Electron Transfer Matrices for UV-MALDI. *J. Am. Soc. Mass Spectrom.* 2017;28(12):2548-2560. https://doi.org/10.1007/s13361-017-1783-z

Cristancho L, Ramírez S, Combariza M, Blanco-Tirado C. (2016). Diseño racional y síntesis de nuevas matrices MALDI de transferencia electrónica basadas en 2,7-dibromofluoreno. Universidad Industrial de Santander,

Descy JP, Gosselain V. Development and ecological importance of phytoplankton in a large lowland river (River Meuse, Belgium). *Hydrobiologia.* 1994;289(1-3):139-155. https://doi.org/10.1007/BF00007415

Field CB. Primary Production of the Biosphere: Integrating Terrestrial and Oceanic Components. *Science*. 1998;281(5374):237-240. https://doi.org/10.1126/science.281.5374.237

Fock V. Näherungsmethode zur Lösung des quantenmechanischen Mehrkörperproblems. *Z. Physik*, 1930;61(1-2):126-148. https://doi.org/10.1007/BF01340294

Giraldo-Dávila D, Chacón-Patiño M, Ramirez-Pradilla J, Blanco-Tirado C, Combariza M. (2018). Selective ionization by electron-transfer MALDI-MS of vanadyl porphyrins from crude oils. Fuel

Godoy D, Ramírez S, Combariza M, Blanco-Tirado C. (2019). Reactividad en fase gaseosa de α-cianofenilenvinilenos como matrices MALDI de transferencia electrónica, Universidad Industrial de Santander.

Gomez DA, Combariza AF, Sastre G. Quantum-chemistry calculations of hydrogen adsorption in MOF-5. *Physical Chemistry Chemical Physics*, 2009;11(40):9250. https://doi.org/10.1039/b909021e

Golbeck JH, van der Est A. (2014). The Biophysics of Photosynthesis. In J. Golbeck & A. van der Est (Eds.), The Biophysics of Photosynthesis. Springer New York. https://doi.org/10.1007/978-1-4939-1148-6

Goupy P, Carail M, Giuliani A, Duflot D, Dangles O, Caris-Veyrat C. Carotenoids: Experimental Ionization Energies and Capacity at Inhibiting Lipid Peroxidation in a Chemical Model of Dietary

Oxidative Stress. *J. Phys. Chem. B*. 2018;122(22):5860-5869. https://doi.org/10.1021/acs.jpcb.8b03447

Hartree DR. The Wave Mechanics of an Atom with a Non-Coulomb Central Field. Part II. Some Results and Discussion. *Math. Proc. Camb. Philos. Soc.* 1928;24(1):111-132. https://doi.org/10.1017/S0305004100011920

Hasegawa K, Noguchi T. Density Functional Theory Calculations on the Dielectric Constant Dependence of the Oxidation Potential of Chlorophyll: Implication for the High Potential of P680 in Photosystem II †. *Biochemistry*. 2005;44(24):8865-8872. https://doi.org/10.1021/bi050273c

Jaramillo P, Coutinho K, Cabral BJC, Canuto S. Ionization of chlorophyll-c2 in liquid methanol. *Chem. Phys. Lett.* 2012;546:67-73. https://doi.org/10.1016/j.cplett.2012.07.040

Jensen F. (2017). Introduction to Computational Chemistry Computational Chemistry. https://doi.org/10.1007/s00214-013-1372-6

Koopmans T. Über die Zuordnung von Wellenfunktionen und Eigenwerten zu den Einzelnen Elektronen Eines Atoms. *Physica*. 1934;1(1-6):104-113. https://doi.org/10.1016/S0031-8914(34)90011-2

Lazzari-Dean J, Krylov AI, Bravaya KB. The effects of resonance delocalization and the extent of ϖ system on ionization energies of model fluorescent proteins chromophores. *Int. J. Quantum Chem.* 2015;115(18):1258-1264. https://doi.org/10.1002/qua.24825

Lewars EG. (2011). *Computational Chemistry: Introduction to the Theory and Applications of Molecular and Quantum Mechanics*. Springer Netherlands. https://doi.org/10.1007/978-90-481-3862-3

McCarley TD, McCarley RL, Limbach PA. Electron-Transfer Ionization in Matrix-Assisted Laser Desorption/Ionization Mass Spectrometry. *Anal. Chem.* 1998;70(20):4376-4379. https://doi.org/10.1021/ac980527i

Müller W, Nager C, Rosmus P. The frozen orbital approximation for calculating ionization energies with application to propane. *Chem. Phys.* 1980;51(1-2):43-48. https://doi.org/10.1016/0301-0104(80)80078-4

Nakato Y, Chiyoda T, Tsubomura H. Experimental Determination of Ionization Potentials of Organic Amines, β-Carotene and Chlorophyll a. Bulletin of the Chemical Society of Japan, 1974;47(12):3001-3005.

Olenina I, Hajdu S, Edler L, Andersson A, Wasmund N, Busch S, Göbel J, et al. (2006). Biovolumes and Size-Classes of Phytoplankton in the Baltic Sea. In Baltic Sea Environment Proceedings (Vol. 106, Issues 0357–2994). http://www.helcom.fi/Lists/Publications/BSEP106.pdf

Neese F. Software update: the ORCA program system, version 4.0. WIREs *Comput Mol Sci*, 2018;8:e1327. https://doi.org/10.1002/wcms.1327),

Neese Frank, Frank Wennmohs, Ute Becker, Christoph Riplinger. "The ORCA Quantum Chemistry Program Package". *J. Chem. Phys.* 2020;152(22):224108.

Persico M, Granucci G. (2018). Photochemistry: A Modern Theoretical Perspective. Springer International Publishing. https://doi.org/10.1007/978-3-319-89972-5

Plakhutin BN. Koopmans' theorem in the Hartree-Fock method. General formulation. *J. Chem. Phys.* 2018;148(9):. https://doi.org/10.1063/1.5019330

Ramachandran KI, Deepa G, Namboori K. (2008). Computational Chemistry and Molecular Modeling: Principles and Applications. Springer Berlin Heidelberg. https://doi.org/10.1007/978-3-540-77304-7

Ramírez S, Combariza M, Blanco-Tirado C. (2019). Rational design, synthesis, characterization and application of phenylenevinylene and fluorene derivatives as novel MALDI matrices, Universidad Industrial de Santander,

Ramírez-Pradilla JS, Blanco-Tirado C, Combariza MY. Electron-Transfer Ionization of Nanoparticles, Polymers, Porphyrins, and Fullerenes Using Synthetically Tunable α-Cyanophenylenevinylenes as UV MALDI-MS Matrices. ACS *Appl. Mater. Interfaces*, 2019a;11(11):10975-10987. https://doi.org/10.1021/acsami.8b22246

Ramírez-Pradilla JS, Blanco-Tirado C, Hubert-Roux M, Giusti P, Afonso C, Combariza MY. Comprehensive Petroporphyrin Identification in Crude Oils Using Highly Selective Electron Transfer Reactions in MALDI-FTICR-MS. *Energ Fuel.* 2019b;33(5):3899-3907. https://doi.org/10.1021/acs.energyfuels.8b04325

Robb MA. (2018). Theoretical Chemistry for Electronic Excited States (12th ed.). Royal Society of Chemistry.

Roy S, Llewellyn C, Egeland ES, Johnsen G. (2012). Phytoplankton Pigments: Characterization, Chemotaxonomy and Applications in Oceanography. In Environmental Chemistry. Cambridge University Press.

Sánchez L MD. (2019). Identificación de Biomarcadores Fitoplanctónicos Utilizando Espectrometría De Masas MALDI TOF Con Matrices De Transferencia Electrónica. Universidad Industrial de Santander.

Siuzdak G. An introduction to mass spectrometry ionization: An excerpt from The Expanding Role of Mass Spectrometry in Biotechnology, 2nd ed.; MCC Press: San Diego, 2005. *J. Assoc. Lab. Autom.* 2004;9(2):50-63. https://doi.org/10.1016/j.jala.2004.01.004

Szabo A, Ostluand NS. (1996). Modern Quantum Chemistry: Introduction to Advanced Electronic Structure Theory.

Szent-Györgyi A. (1968). BIOLOGICAL RELATIONS. In Bioelectronics (pp. 33–50). Elsevier. https://doi.org/10.1016/B978-0-12-680945-9.50007-8

Takaichi S. Carotenoids in Algae: Distributions, Biosyntheses and Functions. *Mar. Drugs*, 2011;9(6):1101-1118. https://doi.org/10.3390/md9061101

Tian H, Yang X, Cong J, Chen R, Teng C, Liu J, et al. Effect of different electron donating groups on the performance of dye-sensitized solar cells. *Dyes Pigm*. 2010;84(1):62-68. https://doi.org/10.1016/j.dyepig.2009.06.014

Triggle DJ, Taylor JB. (2006). Comprehensive Medicinal Chemistry II Volume 5 : ADME-Tox Approaches. In Medicinal Chemistry (Vol. 5). Elsevier Science.

Ulmer L, Mattay J, Torres-Garcia HG, Luftmann H. Letter: The use of 2-[(2E)-3-(4-tert-butylphenyl)-2-methylprop-2-enylidene]malononitrile as a matrix for matrix-assisted laser desorption/ionization mass spectrometry. *Eur J Mass Spectrom.* 2000;6(1):49-52. https://doi.org/10.1255/ejms.329

Vasil'ev YV, Khvostenko OG, Streletskiy AV, Boltalina OV, Kotsiris SG, Drewello T. Electron Transfer Reactivity in Matrix-Assisted Laser Desorption/Ionization (MALDI): Ionization Energy, Electron Affinity and Performance of the DCTB Matrix within the Thermochemical Framework. *J. Phys. Chem. A.* 2006;110(18):5967-5972. https://doi.org/10.1021/jp060568f